

# 3-D Statistical Cancer Atlas-based Targeting of Prostate Biopsy using Ultrasound Image Guidance

Ramkrishnan Narayanan<sup>a</sup>, Dinggang Shen<sup>b</sup>, Christos Davatzikos<sup>b</sup>, E David Crawford<sup>c</sup>, Albaha Barqawi<sup>c</sup>, Priya Werahera<sup>c</sup>, Dinesh Kumar<sup>a</sup> and Jasjit S Suri<sup>a</sup>

<sup>a</sup>Eigen LLC, 13366 Grass Valley Ave., Grass Valley, CA, USA

<sup>b</sup>Section of Biomedical Image Analysis, Department of Radiology,  
University of Pennsylvania, PA, USA

<sup>c</sup> University of Colorado Denver, Anschutz Medical Campus, CO, USA

## ABSTRACT

Prostate cancer is a multifocal disease and lesions are not distributed uniformly within the gland. Several biopsy protocols concerning spatially specific targeting have been reported in urology literature. Recently a statistical cancer atlas of the prostate was constructed providing voxelwise probabilities of cancers in the prostate. Additionally an optimized set of biopsy sites were computed with 94 – 96% cancer detection accuracy using only 6-7 needles. Here we discuss the warping of this atlas to prostate segmented side-fire ultrasound images of the patient. A shape model was used to speed up registration. The model was trained from 38 surfaces of the prostate gland segmented by experts from real patient TRUS images. This training yielded as few as 15-20 degrees of freedom that were optimized to warp the atlas surface to the patient's ultrasound image followed by elastic interpolation of the 3-D atlas.

As a result the atlas is completely mapped to the patient's prostate anatomy along with optimal predetermined needle locations for biopsy. These do not preclude the use of additional biopsies if desired. A color overlay of the atlas is also displayed on the ultrasound image showing high cancer zones within the prostate. Finally current biopsy locations are saved in the atlas space and may be used to update the atlas based on the pathology report. In addition to the optimal atlas plan, previous biopsy locations and alternate plans can also be stored in the atlas space and warped to the patient with no additional time overhead.

**Keywords:** cancer, prostate, registration, atlas, shape

## 1. INTRODUCTION

The Center for Prostate Disease Research (CPDR) estimates that prostate cancer accounts for nearly 30% of cancers affecting males in the United States in 2007.<sup>1</sup> Early diagnosis, however shows that the five year survival rate approaches 100%. Prostate specific antigen (PSA) measured via a blood test and the digital rectal examination (DRE) are the most common methods to screen for prostate cancer. Commonly used TRUS images do not help identify many prostate cancers since isoechoic areas and large variability in sonographic appearances hardly correlate to cancer. While newer methods such as pulse inversion, color and power Doppler, elastography, contrast and harmonic imaging are starting to gain ground, it is still unclear how suspicious regions in these images correlate with localized prostate cancers. Currently localized prostate cancer is diagnosed by tissue confirmation following transrectal ultrasound (TRUS) guided biopsy procedures.

Numerous protocols concerning biopsy have been discussed, and in particular several modifications to the popular sextant biopsy<sup>2</sup> have been reported. Paul *et al.*<sup>3</sup> added two additional median cores on both sides to compare a ten core biopsy with their modified sextant biopsy reporting 32% and 40% for six and ten cores respectively. Often times, 15 cores are used leading to rectal bleeding, hematuria and hematospermia with negligible improvement in detection rates. Naughton *et al.*<sup>4</sup> reported that only increasing the number of cores from six to twelve did not lead to any improvement. Chen *et al.*<sup>5</sup> reported a 11-core multi-site biopsy including

---

Further author information: (Send correspondence to R. Narayanan)  
R. Narayanan: E-mail: ram.narayanan@eigen.com, Telephone: 1 530 274 1240 Extn: 210

1 sextant, 1 posterior midline, 2 transition and 2 anterior horn cores improving detection rates to 85% and 70% in prostates less than 50g and greater than 50g respectively hinting the importance of targeting specific spatial locations within the prostate. A 3-D prostate model was constructed in<sup>6</sup> showing the distribution of prostate cancer in various zones. Opell *et al.*<sup>7</sup> developed a spatial distribution map of cancers in the prostate concluding that the cancers are more commonly found in the posterior half, apical and mid regions of the prostate and suggesting its use to develop sophisticated biopsy protocols. A six core systematic core biopsy (SRSCB) technique is commonly used<sup>2</sup> because of its better sampling independent of tumor echogenicity. Shen *et al.*<sup>8</sup> constructed the first probabilistic atlas of cancers within the prostate showing voxel-wise probability of cancer. This work was further improved upon in<sup>9</sup> where a pre-computed optimal biopsy scheme in the atlas space consisting of 6-7 needles promised 96-97% cancer detection accuracy.

The cancer atlas, constructed from a large cohort of expert annotated prostatectomy specimen is capable of providing voxel based comparison of cancer probabilities throughout the prostate. While this advanced protocol for biopsy is a marked improvement over current methods, its applicability is limited by how fast the entire 3-D atlas or biopsy locations can be mapped to the patient's ultrasound image to aid the urologist in selecting needle locations. In our work here we discuss the fast warping of the cancer atlas to the subject using a principal component analysis based shape model trained from a large database of expert segmented side-fire ultrasound images of the prostate. The off-line training results in 15-20 basis vectors accounting for more than 95% variance of the entire training set. The atlas, defined within the mean surface of this model is warped to the subject via the optimization of the projections on the basis vectors. The shape model is thus used to register the mean surface to the segmented subject surface. The point correspondences between the mean surface and its optimal warp to the subject are used as boundary conditions to elastically interpolate<sup>10</sup> the entire 3-D atlas volume to the patient's TRUS image. The optimal pre-computed needle positions in the atlas space are also consequently mapped to the patient's space showing the statistically independent locations with highest probability of detecting cancer. The atlas was validated by registering it to 3D reconstructed histology images with expert annotated ground truths. The detection rate for 7 and 12 core optimized biopsy protocols were found to be 84.81% and 89.87% respectively.

## 2. METHOD

Atlas based planning is one of several tasks that make up the biopsy workflow. During biopsy, it is essential to know the prostate boundary as well as the precise location of the needle. Therefore, information about intra-procedural prostate location and needle tracing is crucial for such a target-directed biopsy scheme. The interventional device from Eigen LLC includes a mechanical assembly that provides real-time locations of the probe so that the patient's prostate and the biopsy needle are well referenced in situ. Subjective mental formatting to deduce information in the third dimension from 2-D slices is replaced by simple navigation in the computer generated 3-D space. A standardized prostate biopsy workflow consists of the following three phases:

1. "Ground" scan to acquire a 2-D image stack covering the entire gland using a traditional ultrasound probe and machine. This scan can be accomplished within six seconds with Eigen's device.
2. Reconstruction and display of the 3-D prostate gland from the 2-D image stack. Accurate tracking of the positions of the 2-D slices and 3-D segmentation are needed to delineate the boundary of the gland. Following this, the user can choose any one or more of the following schemes to plan targets.
  - a) Conventional 6, 8, 10, and 16-core biopsy schemes.
  - b) Urologist-input via computer mouse or keyboard.
  - c) Previously optimized core site locations estimated by cancer probability atlas mapped to the patient
  - d) Repeat biopsy by references of previous biopsy locations.
3. Accurate sampling of the targeted regions with 3D image guidance and tracking.

The cancer atlas is a 3D image consisting of cancer probabilities at every voxel. The absence of anatomical information in the atlas space precludes its registration directly with patient's TRUS images. Additionally intensity based registration could take long registration times delaying biopsy planning. Instead, the prostate

gland is segmented from TRUS images via a semiautomatic strategy using the method described in.<sup>11</sup> In this method the authors use a discrete dynamic contour (DDC) to segment capsule boundaries based on edge gradients, contour smoothness and a damping force related to the contour velocity. The segmentation is performed on a 2D plane rotated about the anterior-posterior axis at the center of the image containing the prostate. Each plane is segmented one at a time before obtaining a new plan view spaced an an angle of 3 degrees about the axis. Segmentation of the prostate gland typically takes 8 seconds on a 3.2 GHz Pentium 4 with 3 Gb system memory.

The atlas is aligned to the TRUS image by interpolating the boundary correspondences of the segmented prostate gland and the statistical mean surface estimated via shape based registration. There are two offline steps involved in the atlas warping procedure:

- **Collection of Cancer Statistics:** This step was completed by our collaborators where a detection rate of 94 – 96% was achieved using only 6-7 biopsy cores. See.<sup>8,9</sup> The following is a brief summary of their effort. 157 prostatectomy specimen from the center for prostate disease research (CPDR) tissue bank were used in the preparation of the atlas. They were whole mounted and step sliced at 2.25 mm. 5  $\mu$ m thick sections were then stained with haematoxylin and eosin. These specimen were pathologically reviewed for tumors by an expert, reconstructed in 3D and labeled based on cancers and normal tissue.
- **Training of Prostate Shape Model:** A statistical shape model of the prostate was constructed using 38 expert segmented surfaces from real patient TRUS images as described by Cootes *et al.*<sup>12</sup> Expert segmented prostate surfaces from TRUS images were non-linearly registered using AFDM<sup>13</sup> providing vertex correspondences from a chosen model to each of the other surfaces. Then variations due to global scale, rotation and translation were removed, and the Eigenvalues and Eigenvectors for the set of aligned shapes,  $D = [\mathbf{x}_{s1} \mathbf{x}_{s2} \dots \mathbf{x}_{sN}]$ , where  $\mathbf{x}_{si}$  is a vector containing all the vertices of the  $i$ th surface, were computed. Any model conforming shape could thus be described as  $\mathbf{x}_s = \bar{\mathbf{x}}_s + \sum_{i=1}^M \alpha_i \mathbf{v}_i$ , where  $\bar{\mathbf{x}}_s$  is the mean shape,  $\mathbf{v}_i$  is the  $i$ th Eigenvector,  $\alpha_i$  is the set of projections on each Eigenvector, and  $M$  is the number of the Eigenvector used in the shape basis after sorting the vectors in descending order of Eigenvalues.  $M$  was picked so as to account for over 95% of the training data.

Biopsy planning would have to be done in the patient's TRUS image space which requires that the atlas is fully registered to it. The online atlas warping procedure consists of two steps

- **Segmentation and Surface Registration:** The patient's TRUS image is semi-automatically segmented using the method described earlier. This is followed by registration of the statistical mean surface (within which the 3D atlas is defined) from the shape model to the patient's segmented surface. This is accomplished via optimization of projections on Eigenvectors to produce model compliant warps of the mean to maximize its similarity with the segmented subject surface ( $\mathbf{y}$ ) as follows:

$$(\hat{\alpha}, \hat{\mathbf{t}}, \hat{R}, \hat{c}) = \arg \min_{(\alpha, \mathbf{t}, R, c)} \|cR(H\alpha + \bar{\mathbf{x}}_s) + \mathbf{t} - \mathbf{y}\|, \quad (1)$$

where  $\mathbf{t}$ ,  $R$  and  $c$  are the global translation, rotation and scale parameters, and  $H = [\mathbf{v}_1 \mathbf{v}_2 \dots \mathbf{v}_N]$  is the matrix of Eigenvectors.

- **Elastic Warping:** To warp the 3-D Atlas volume to the patient's TRUS image using surface correspondences established from the previous step using the method described in.<sup>10</sup> The forces on the mean surface elastically drives the flow to warp the entire atlas volume to align with the patient's TRUS image.

The online steps assume that the patient's TRUS image has already been segmented for the prostate gland. Alternately the shape model may be directly used to segment the prostate gland by producing model compliant warps that align along the edges of the gland in the TRUS image. Figure 1 shows both offline and online steps in the algorithm. Figure 2 shows the atlas overlaid on the patient's TRUS image and Figure 3 shows optimal needle locations after atlas registration on patient's segmented surface from TRUS.

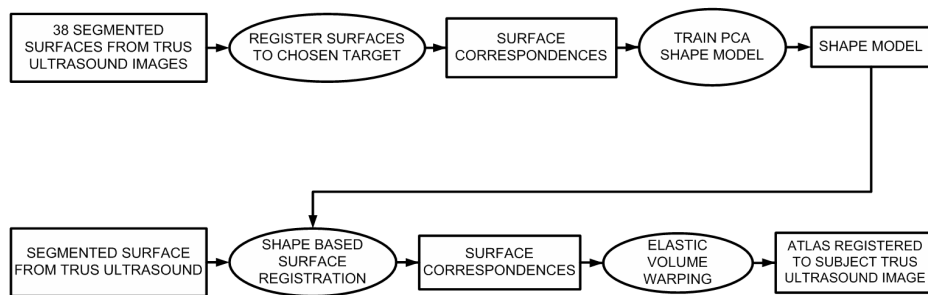


Figure 1. Top: Offline training of the shape model. Bottom: Online registration of the atlas to the patient's TRUS image.

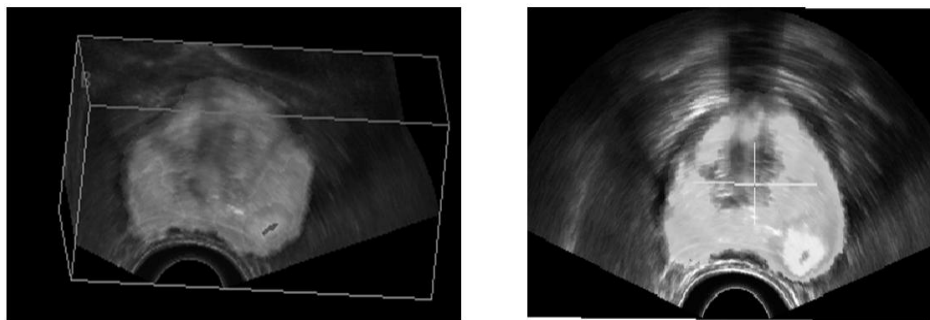


Figure 2. Both images show atlas overlaid on the patient's TRUS image. A color overlay of 3D statistical cancer probabilities on the TRUS images may be used to pick target sites for biopsy.

### 3. RESULTS

The surface registration of the mean shape with the segmented surface yielded a high volume intersection-union ratio averaging 0.87 after registration with 20 subjects. The atlas cancer detection rate is difficult to assess by registering it to TRUS images. This is because cancers often isoechoic in TRUS making it impossible to annotate precise cancer boundaries. As a result the atlas was registered instead to 3D reconstructed data from prostatectomy specimen. The histological sections for these specimens were outlined on prostate boundaries and cancerous regions. These sections were then fully reconstructed to 3D. The 3D shape based atlas registration was validated by registering it to these 3D images with cancers annotated. The detection rate after registration for 7 and 12 core biopsy was found to be 84.81% and 89.87% respectively.

### 4. CONCLUSION

The cancer detection rate for 7 and 12 core biopsy protocols was found to be high. Future work would involve comparing the detection rate of these protocols with popular biopsy protocols, e.g. sextant, extended 12 core systematic biopsy. The registration took approximately 30 seconds on a Pentium Core 2 Duo (2.67 GHz) with 2 Gb system memory. Initial results in terms of both speed of atlas based registration and the detection rate appear promising. The main disadvantage of using radical prostatectomy specimen is that cancer was previously detected in these men by six core random systematic core biopsy, lesion directed or repeat biopsies. As a result the data may likely be biased. Kawata *et al*<sup>14</sup> proposed using autopsy prostates that represent a subset of the population whose diseases were not diagnosed prior to death. Further they classify carcinomas as clinically threatening if they had a volume greater than 0.5 cc and/or a Gleason sum greater than or equal to 7. Newer sophisticated atlases with high clinically significant detection rate tested against autopsy data may provide valuable insight to help guide biopsy to regions statistically shown to develop disease. Our registration method can be straightforwardly used with newer atlases with no change to the existing set up. Elastic warping may

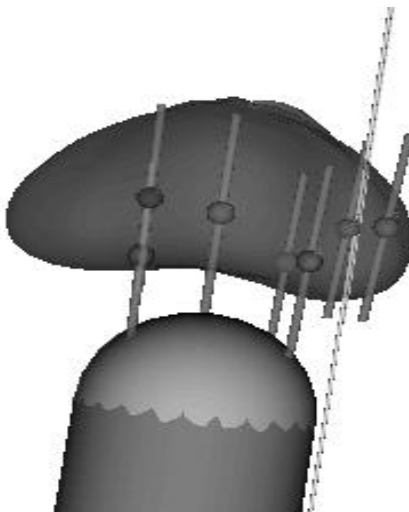


Figure 3. Shows probe, needle trajectory, and optimized 7-core biopsy configuration on patient's rendered surface from segmentation.

be performed via parallel relaxation making it highly amenable to parallelization on a graphical processing unit (GPU) to speed up implementation. The existing atlas could also be updated based on clinical detection results from the pathology report. Future work will involve measuring and potentially improving the sensitivity and specificity of our cancer atlas using autopsy data.

The optimized biopsy in the patient space may be used by the urologist as a target site during planning. Alternately the color overlaid Atlas on the TRUS image could be used to guide target selection. These however, do not preclude selection of additional sites by the urologist. The pathology report on cancers detected at various biopsy sites may be used to update the atlas periodically. Since the atlas is described in the mean shape of the shape model, standard biopsy plans may also be defined on this template shape that are automatically driven to register to TRUS during elastic warping thus enabling definition of popular biopsy plans in the atlas space.

## REFERENCES

1. A. Jemal, R. Siegel, E. Ward, T. Murray, J. Xu, and M. J. Thun, "Cancer statistics 2007," *CA Cancer J Clin*, 2007.
2. K. K. Hodge, J. E. McNeal, M. Terris, and T. A. Stamey, "Random systematic versus directed ultrasound-guided transrectal core biopsies of the prostate," *J Urol*, 1989.
3. R. Paul, S. Scholer, H. van Randerborgh, H. Kubler, M. Alschibaja, R. Busch, and R. Hartung, "Optimization of prostatic biopsy: A prospective randomized trial comparing the sextant biopsy with a 10-core biopsy impact of prostatic region of sampling," *Urol Int* **74**, pp. 203–208.
4. C. K. Naughton, D. C. Miller, D. E. Mager, D. K. Ornstein, and W. J. Catalona, "A prospective randomized trial comparing 6 versus 12 prostate biopsy cores: impact on cancer detection," *J Urol*. **164**, pp. 388–392.
5. M. E. Chen, P. Troncso, K. Tang, R. J. Babaian, and D. Johnston, "Comparison of prostate biopsy schemes by computer simulation," *J Urol*. **53**, pp. 951–960.
6. M. B. Opell, J. Zeng, J. J. Bauer, R. R. Connelly, W. Zhang, I. A. Sesterhenn, S. K. Mun, J. W. Moul, and J. H. Lynch, "Modeling and mapping of prostate cancer," *Computers and Graphics* **24**, pp. 683–694, 2000.
7. M. B. Opell, J. Zeng, J. J. Bauer, R. R. Connelly, W. Zhang, I. A. Sesterhenn, S. K. Mun, J. W. Moul, and J. H. Lynch, "Investigating the distribution of prostate cancer using three-dimensional computer simulation," *Prostate Cancer and Prostatic Diseases* **5**, pp. 204–208, 2002.
8. D. Shen, Z. Lao, J. Zeng, W. Zhang, I. A. Sesterhenn, L. Sun, J. W. Moul, E. H. Herskovits, G. Fichtinger, and C. Davatzikos, "Optimized prostate biopsy via a statistical atlas of cancer spatial distribution," *Medical Image Analysis* **8**, pp. 139–150, 2004.

9. Y. Zhan, D. Shen, J. Zeng, L. Sun, G. Fichtinger, J. Moul, and C. Davatzikos, "Targeted prostate biopsy using statistical image analysis," *IEEE Trans. Med. Imag.* **26**(6), pp. 779–788, 2007.
10. C. Davatzikos, "Spatial transformation and registration of brain images using elastically deformable models," *Comp. Vision and Image Understanding* **66**(2), pp. 207–222, 1997.
11. H. M. Ladak, F. Mao, Y. Wang, D. B. Downey, D. A. Steinman, and A. Fenster, "Prostate boundary segmentation from 2d ultrasound images," *Engg. in Medicine and Biology Society, Proc of the 22nd Annual Int. Conf. of IEEE* **4**, pp. 3188–3191, 2000.
12. T. F. Cootes, C. J. Taylor, D. H. Cooper, and J. Graham, "Active shape models - their training and application," *Computer Vision and Image Understanding* **61**(1), pp. 38–59, 1995.
13. D. Shen and C. Davatzikos, "An adaptive-focus deformable model using statistical and geometric information," *IEEE Trans. on Pattern Anal. and Machine Intelligence* **22**(7), pp. 1–8, 2000.
14. N. Kawata, G. J. Miller, E. D. Crawford, K. C. Torkko, J. S. Stewart, M. S. Lucia, H. L. Miller, D. Hirano, and P. N. Werahera, "Laterally directed biopsies detect more clinically threatening prostate cancer: Computer simulated results," *The Prostate* **57**, pp. 118–128, 2003.